

# Fault zone architecture and permeability structure

Jonathan Saul Caine Department of Geology and Geophysics, University of Utah, Salt Lake City, Utah 84112  
James P. Evans Department of Geology, Utah State University, Logan, Utah 84322-4505  
Craig B. Forster Earth Sciences and Resources Institute, Department of Civil and Environmental Engineering, University of Utah, Salt Lake City, Utah 84112

## ABSTRACT

**Fault zone architecture and related permeability structures form primary controls on fluid flow in upper-crustal, brittle fault zones. We develop qualitative and quantitative schemes for evaluating fault-related permeability structures by using results of field investigations, laboratory permeability measurements, and numerical models of flow within and near fault zones. The qualitative scheme compares the percentage of the total fault zone width composed of fault core materials (e.g., anastomosing slip surfaces, clay-rich gouge, cataclastite, and fault breccias) to the percentage of subsidiary damage zone structures (e.g., kinematically related fracture sets, small faults, and veins). A more quantitative scheme is developed to define a set of indices that characterize fault zone architecture and spatial variability. The fault core and damage zone are distinct structural and hydrogeologic units that reflect the material properties and deformation conditions within a fault zone. Whether a fault zone will act as a conduit, barrier, or combined conduit-barrier system is controlled by the relative percentage of fault core and damage zone structures and the inherent variability in grain size and fracture permeability. This paper outlines a framework for understanding, comparing, and correlating the fluid flow properties of fault zones in various geologic settings.**

## INTRODUCTION

Brittle fault zones are lithologically heterogeneous and structurally anisotropic discontinuities in the upper crust. They may act as conduits, barriers, or combined conduit-barrier systems that enhance or impede fluid flow (Randolph and Johnson, 1989; Smith et al., 1990; Scholz, 1990; Caine et al., 1993; Forster et al., 1994; Antonellini and Aydin, 1994; Newman and Mitra, 1994; Goddard and Evans, 1995). Fault zones are composed of distinct components: a fault core where most of the displacement is accommodated and an associated damage zone that is mechanically related to the growth of the fault zone (Sibson, 1977; Chester and Logan, 1986; Davison and Wang, 1988; Forster and Evans, 1991; Byerlee, 1993; Scholz and Anders, 1994). The amount and distribution of each component control fluid flow within and near the fault zone.

Insufficient data, particularly field-based data, are available to adequately characterize and compare architecture, permeability structure, fluid flow, and mechanical properties of fault zones found in different geologic environments. Current demands to prove the long-term integrity of waste-disposal facilities, produce hydrocarbons from reservoirs compartmentalized by fault zones, extract mineral deposits, and estimate earthquake risk require incorporating detailed, field-based representations of the physical properties of fault zones in predictive fluid flow simulators. Development of valid flow models is hindered by our inability

to measure in situ fault zone properties in a way that adequately characterizes the spatial and temporal variations in permeability, porosity, and storativity.

In this paper, we compile data, terminology, and conceptual models in order to consolidate our knowledge of fault-related permeability structures. We outline a fault zone model and a set of indices that serve as a guide in evaluating the physical properties of fault zones. This model can be used as a framework for determining spatial variability in fault zone architecture from field data and for incorporating physically based geologic information in mathematical models of fluid flow in faulted rocks. We first define

the major components of a fault zone and then set forth both qualitative and quantitative schemes for fault-related permeability structures. The schemes are based on a synopsis of our research and the work of other authors (Sibson, 1981; Oliver, 1986; Chester and Logan, 1986; Parry and Bruhn, 1986; Scholz, 1987; Scholz and Anders, 1994; Parry et al., 1988; Bruhn et al., 1990; Smith et al., 1990; Forster and Evans, 1991; Moore and Vrolijk, 1992; Caine et al., 1993; Newman and Mitra, 1994; Goddard and Evans, 1995).

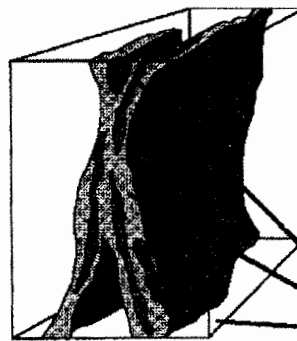
## FAULT ZONE DEFINITION

The primary components of upper-crustal fault zones are fault core, damage zone, and protolith (shown in the conceptual model of Fig. 1). No scalar relationship is implied between the components, nor must all of the components be present in any given fault zone. Note that the fluid flow properties of a fault zone may change, thus the diagram represents only a single point in time. For example, the core may act as a conduit during deformation and as a barrier when open pore space is filled by mineral precipitation following deformation. Thus, it is important to specify the stage of fault evolution when forming a conceptual model for a particular fault zone.

We define a fault core as the structural, lithologic, and morphologic portion of a fault zone where most of the displacement is

### FAULT ZONE ARCHITECTURAL COMPONENTS

- FAULT CORE
  - Gouge
  - Cataclastite
  - Mylonite
- ▨ DAMAGE ZONE
  - Small faults
  - Fractures
  - Veins
  - Folds
- PROTOLITH
  - Regional structures



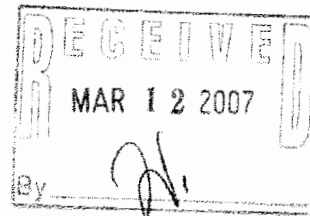
### FACTORS CONTROLLING $k$

- Lithology
- Fault scale
- Fault type
- Deformation style & history
- Fluid chemistry
- P-T history
- Component percentage
- Component  $k$
- Component anisotropy (magnitude & direction of  $k_{max}$  &  $k_{min}$ )



Figure 1. Conceptual model of fault zone with protolith removed (after Chester and Logan, 1986; Smith et al., 1990). Ellipse represents relative magnitude and orientation of the bulk two-dimensional permeability ( $k$ ) tensor that might be associated with each distinct architectural component of fault zone.

Data Repository item 9659 contains additional material related to this article.



14673

accommodated (Fig. 1). Fault cores may include single slip surfaces (Caine et al., 1991), unconsolidated clay-rich gouge zones (Anderson et al., 1983), brecciated and geochemically altered zones (Sibson, 1977), or highly indurated, cataclasite zones (Chester and Logan, 1986). Our field-based observations suggest that thickness variations, both down dip and along strike, combined with a distinctive internal structure and composition, play an important role in controlling the fluid flow properties of fault zone cores. Grain-size reduction and/or mineral precipitation generally yield fault cores with lower porosity and permeability than the adjacent protolith (e.g., Chester and Logan, 1986; Antonellini and Aydin, 1994; Goddard and Evans, 1995). Permeability reduction leads to fault cores that act as barriers to fluid flow (see Table 1 below).

A damage zone is the network of subsidiary structures that bound the fault core and may enhance fault zone permeability relative to the core and the undeformed protolith (Fig. 1; Chester and Logan, 1986; Smith et al., 1990; Andersson et al., 1991; Scholz and Anders, 1994; Goddard and Evans, 1995). Fault-related subsidiary structures in damage zones include small faults, veins, fractures, cleavage, and folds that cause heterogeneity and anisotropy in the permeability structure and elastic properties of the fault zone (Bruhn et al., 1994). Wide damage zones may indicate multiple episodes of slip and the overprinting of successive deformation events.

The fault core and damaged zones shown in Figure 1 are surrounded by relatively undeformed protolith. This is the country rock where fault-related permeability structures are absent, and both fluid flow and elastic properties of the rock reflect those of the unfaulted host rock. Fault zone architecture may ultimately reflect the degree to which the processes of strain localization vs. strain distribution compete as the fault zone cuts different rock types in the protolith.

The geometry and magnitude of permeability contrasts between the fault core and damage zone are primary controls on the barrier-conduit systematics of the fault zone. Fracture density in the fault core is usually significantly less than in the damage zone (Andersson et al., 1991; Chester et al., 1993). Thus, the permeability of the fault core may be dominated by the grain-scale permeability of the fault rocks, whereas the damage zone permeability is dominated by the hydraulic properties of the fracture network.

#### CONCEPTUAL SCHEME FOR FAULT-RELATED FLUID FLOW

A range of fault zone architectures are observed in outcrop (Fig. 2). Each of the four end-member architectural styles is associated with a characteristic permeability structure (Chester and Logan, 1986; Bruhn et al., 1990; Forster and Evans, 1991; Moore and Vrolijk, 1992; Newman and Mitra, 1994). These include localized conduits, distributed conduits, localized barriers, and combined conduit-barriers (Table 1).

#### NUMERICAL MEASURES OF FAULT ZONE ARCHITECTURE AND PERMEABILITY STRUCTURE

Fault zone architecture and permeability structure are characterized by using three numerical indices derived from our conceptual model:  $F_a$ ,  $F_m$ , and  $F_s$ .

$$F_a = \frac{\text{damage zone width}}{\text{total fault zone width}}$$

$$= \frac{\text{damage zone width}}{\text{core width} + \text{damage zone width}}$$

$F_m$  = mean of  $F_a$  values for a single fault zone.

$$F_s = (F_a)_{\max} - (F_a)_{\min}$$

$F_a$  is a fault zone architectural index. Values of  $F_a$  range from 0 to 1 and provide a mea-

sure of the relative width of the fault core and damage zone at a specified location (Fig. 3A). When  $F_a$  is 0, ideally the damage zone is absent, and the lower permeability of the fault core causes the fault zone to act as a barrier to flow. When  $F_a$  is 1, ideally the fault core is absent, and the presence of a higher permeability damage zone causes the fault zone to act as a conduit for flow.  $F_m$  is the mean value of  $F_a$  obtained for a set of fault zone measurements (Fig. 3A).  $F_m$  is indicative of the overall architecture and permeability structure of a fault zone and can be measured along specific transects (e.g., along the dip or strike of the fault zone).  $F_s$  is a spatial variability index that represents the spread in values of  $F_a$  obtained within a specific fault zone (Fig. 3A). This measure of the spread is, perhaps, a more physically based measure than using the standard deviation.

Plotting values of  $F_a$  against total fault zone width yields insight regarding the mechanics of faulting, the response of protolith rock types to deformation, and the resulting architecture and permeability structure within a single fault zone (Fig. 3A) or within a group of fault zones (Fig. 3B).<sup>1</sup> The horizontal axis of the plot ranges between two end-member architectures and permeability structures. When  $F_a = 0$ , the architecture of the fault zone may be dominated by strain localized deformation resulting in a barrier-type permeability structure (Fig. 3). When  $F_a = 1$ , the fault zone may reflect distributed strain resulting in a conduit-type permeability structure (Fig. 3). Intermediate values of  $F_a$  indicate combined strain localization and distributed deformation that yield a barrier-conduit permeability structure (Fig. 3).

Figure 3A is an example plot of fault zone architecture and permeability structure obtained for a single fault (fault 6) located in upper Paleozoic clastic rocks at Traill Ø, East Greenland. Fault 6 is an oblique-slip normal fault on which there has been 85 m of displacement. Excellent exposures of the fault core, damage zone, and protolith were mapped at 11 localities along a 400 m vertical traverse. Numbers associated with each point plotted in Figure 3A indicate the elevation at which the data were collected.

Figure 3A shows possible correlations between protolith rock type, the protolith's mechanical response to deformation, and the resulting permeability structure of fault 6. The three points clustered in the lower right-hand corner of Figure 3A are from a part of fault 6 where the protolith is domi-

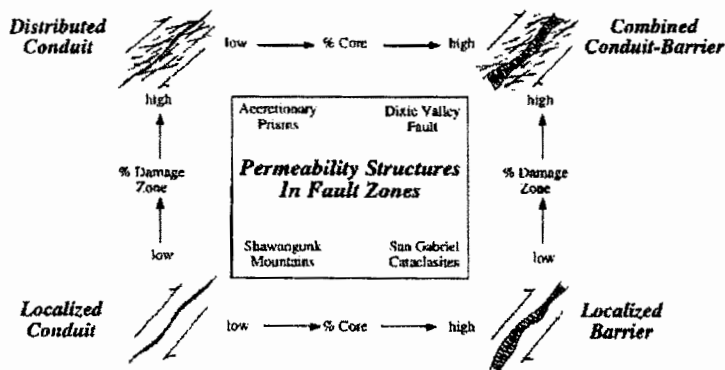


Figure 2. Conceptual scheme for fault-related fluid flow.

<sup>1</sup>GSA Data Repository item 9659, raw fault-zone data, is available from Documents Secretary, GSA, P.O. Box 9140, Boulder, CO 80301. E-mail: editing@geosociety.org.

**TABLE 1. FAULT ZONE ARCHITECTURAL STYLES AND PERMEABILITY STRUCTURES**

| Permeability structure   | Architectural style   | Fault core   | Damage zone   | Examples   | Applicable flow model   |
|--------------------------|---|--|---|--|---|
| Localized conduit        | Localized slip along a single curvilinear surface or along discretely segmented planes.                     | Absent to poorly developed.  | Absent to poorly developed.   | Small faults in Shawangunk Mountains of eastern New York (Caine et al., 1991). | Discrete fractures modeled as conduits with parallel walls.   |
| Distributed conduit      | Distributed slip developed along distributed surfaces and fractures.  | Absent to poorly developed as narrow, discrete, and discontinuous bands. | Well-developed discrete slip surfaces and associated fracture networks. | Modern accretionary prisms (Moore and Vrolijk, 1992).                          | Equivalent porous medium.   |
| Localized barrier        | Localized slip accommodated within cataclastic zone.  | Well-developed fault core cataclases.                                    | Absent to poorly developed.   | Deformation bands in sandstones (Antonellini and Aydin, 1994).                 | Aquifer (fault core) within a higher-permeability aquifer (protolith).  |
| Combined conduit-barrier | Deformation accommodated within a localized cataclastic zone and distributed zone of subsidiary structures. | Well-developed fault core cataclases.                                    | Well-developed discrete slip surfaces and associated fracture networks. | Dixie Valley normal fault, Dixie Valley, Nevada (Bruhn et al., 1994).          | Aquifer (fault core) sandwiched between two aquifers (damage zone) with $k_{max}$ within and $k_{min}$ normal to the plane of the fault zone. |

nated by shale and the fault core lithology is dominated by clay-rich gouge. The damage zone structures include quartz and calcite veins, open fractures, and small faults. Outcrop observations suggest that where the fault zone cuts shale-rich protolith there has been a higher degree of strain localization than where it cuts sandstone-rich protolith. This is illustrated by the clustering of points in contrast to the more diffusely distributed points. The high clay content in the fault core in this part of the fault, combined with veins and open fractures in the damage zone, would suggest that the fault zone acted as a syn- and postdeformational conduit-barrier permeability structure.

The relatively wide spread of the diffusely distributed points corresponds to the increase of quartz-rich sandstone in the protolith. At these locations the fault core lithology becomes dominated by silicified breccias. The fault zone architecture and permeability structure in this region indicates that the fault zone would have been a

syndepositional flow conduit and a post-deformational conduit-barrier fluid flow system, with flow being preferentially oriented parallel to the fault zone.

For fault 6,  $F_m = 0.79$  (Fig. 3A). This result indicates that the overall architecture is a conduit-barrier fluid flow system, which agrees with outcrop observations. Both silicified breccia and clay-rich gouge in the core would act as barriers to flow normal to the fault zone, and open fractures in the damage zone would act as a conduit for flow parallel to the fault zone. The overall spread in values of  $F_a$  obtained for fault 6 yields an  $F_s$  value of 0.33. This relatively small value of  $F_s$  suggests that fault 6 has a relatively uniform architecture, which is observed in the field.

Fault zone architecture and permeability structure plots can also be used with three-dimensional data from extensive surface exposures and drill cores. Multiple fault zones from a single area or many different areas can be plotted to compare lithology, defor-

mation structures, and fluid flow properties (Fig. 3B). Figure 3B shows values of  $F_m$  plotted for several different fault zones where we have obtained data from our field work or from the literature. The data shown in Figure 3B suggest that fault zones that are damage zone dominated (e.g.,  $F_m$  values greater than 0.5) tend to form in clastic rocks and span a large range of displacements. Plotting architectural data and determining  $F_m$  from many diverse fault zones will enable correlations to be made between the factors that control fault zone architecture (e.g., lithology, displacement, and degree of strain localization) and subsequent fluid flow properties (Fig. 3B). By using this approach, a better understanding of the "rules" that govern the development of fault zone architecture and permeability structure may be gained, and predictive estimates of the fluid flow properties of similar fault zones might be made where direct measurements are not possible.

**DISCUSSION: FACTORS THAT CONTROL FAULT ZONE HYDROGEOLOGY**

Intrinsic controls (i.e., rock types vs. extrinsic controls such as stress state) on fault zone permeability, porosity, and storativity include lithology, fault displacement, three-dimensional fault zone geometry, deformation conditions, types of subsidiary structures, fluid-rock interactions, and the spatial and temporal variability of these parameters. Little work using field-based and experimental methods has been done to gain insight into these controls. A major difficulty in assessing fault zone permeability data comes from the lack of consistent documentation of the morphological position (i.e., core, damage zone, or protolith) from which fault zone samples and data are collected (Evans, 1990). Fully characterizing the fluid flow properties of fault zones involves obtaining permeability data for each fault zone component and clearly documenting the

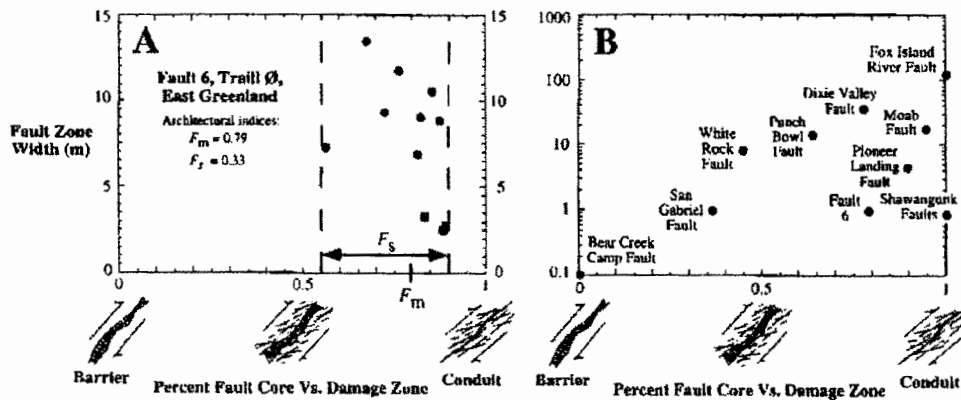


**Figure 3. Fault zone architecture and permeability structure plots. A: Data obtained from fault 6, Trail Ø, East Greenland (dots represent quartz-rich lithologies; squares represent clay-rich lithologies). B: Data from faults mapped in different geologic environments.**

component of the fault zone from which samples and related data are collected.

Field observations of unfractured fault core materials suggest that they are dominated by grain-scale permeability. Laboratory-determined permeabilities for natural fault core materials show a range of variation of approximately 10 orders of magnitude ( $10^{-12}$  to  $10^{-22}$  m<sup>2</sup> from Smith et al., 1990). These data suggest that the permeability of fault core materials depends, in part, on lithology and the degree to which that lithology has been chemically altered. Rocks with the lowest phyllosilicate content tend to have the highest permeability. If there is a direct correlation between protolith rock type and the types of fault core materials that develop in a given deformation environment, then a predictive link may be made with the resulting conduit-barrier systematics.

Although fault zone core materials often have low matrix permeability, they may not always act as a barrier to flow, particularly during deformation. For example, work on the Dixie Valley fault zone shows that the fault core acted as a short-lived, syndeformational, fluid flow conduit that then rapidly sealed to form a barrier to flow. This history is also indicated from work on fault 6, Traill Ø, East Greenland. In contrast, damage zones tend to be conduits compared with both the fault core and the often lower or "background" permeability of the protolith.

In spite of the dearth of laboratory-determined grain-scale permeability values from samples of damage zone materials, our field observations suggest that damage zone permeability is fracture dominated. The juxtaposition of highly fractured damage zone materials with undeformed protolith and generally unfractured fault core materials forms major permeability contrasts within a fault zone. Preliminary estimates of damage zone fracture permeability, using the fracture-permeability estimation methods of Oda et al. (1987) and Bruhn (1993), in both the Dixie Valley fault zone and fault 6, are two to three orders of magnitude greater than the permeability of fractured protolith and four to six orders of magnitude greater than the fault core grain-scale permeabilities. The magnitude and spatial variability of this permeability contrast may be the primary control on fault zone barrier-conduit systematics.

Additional controls on fault zone architecture and permeability structure may include deformation conditions and the chemistry of fault zone fluids. Understanding the combined impact of mechanical and chemical changes in each of the three fault zone components on overall architecture and permeability structure is crucial to a better un-

derstanding of heterogeneity and anisotropy in fault zones. Field-based fault zone architectural data can then be evaluated in the context of permeability structure and formative deformation processes by using the quantitative scheme and architectural indices.

## CONCLUSIONS

Fluid flow in upper-crustal, brittle fault zones depends on fault zone architecture and permeability structure. We represent these aspects of fault zone structure and hydrogeology in the qualitative and quantitative schemes presented in this paper. The schemes are based on a three-component fault zone model that includes a fault core, damage zone, and protolith. This conceptual model is used to delineate the distinct structural and hydrogeologic regimes of a fault zone. A conceptual scheme with four end members is used to identify the range of possible and observed configurations of the three fault zone components. A second, more quantitative scheme, represents variations in fault zone structure by using architectural indices. Adopting these schemes provides a consistent framework for evaluating how the permeability structure of fault zones controls fluid flow in diverse structural regimes.

There is a clear need to continue field-based characterization and sample collection to determine the factors that control fluid flow in fault zones. This work should be done in each fault zone component, on a variety of fault zone types developed within different lithologies over a broad range of scales. Once refined quantitative data are added to the scheme, new axes may be added. These might include time or lithology axes that would make the schemes more comprehensive and possibly provide a predictive tool for better understanding fault zone architecture and permeability structure. The role of fluids in faulting processes, as well as the growing concerns of fault-related utilization of ground-water, hydrocarbon, mineral, and geothermal resources, makes understanding and characterizing fault zone architecture and permeability structure critical at various times throughout the evolution of a fault zone.

## ACKNOWLEDGMENTS

We thank Arild Andresen of the University of Oslo for support of field work in East Greenland, Exxon Production Research Company for support of field and laboratory work in east Greenland, U.S. Geological Survey National Earthquake Hazards Reduction Program grant 1434-93-G-2280 (to Forster, R. L., Bruhn, and J. Fredrich) for support of work on the Dixie Valley fault zone, and National Science Foundation grant 92-05774 and U.S. Geological Survey National Earthquake Hazards Reduction Program grant 1434-94-G-2468 (to Evans).

## REFERENCES CITED

Anderson, L. J., Osborne, R. H., and Palmer, D. F., 1983, Cataclastic rocks of the San Gabriel fault—An expression of deformation at deeper crustal levels in the San Andreas fault zones: *Tectonophysics*, v. 98, p. 209–251.  
Anderson, J. E., Ekman, L., Nordqvist, R., and Winberg, A., 1991,

Hydraulic testing and modeling of a low-angle fracture zone at Finnsjön, Sweden: *Journal of Hydrology*, v. 126, p. 45–77.  
Antonellini, M., and Aydin, A., 1994, Effect of faulting on fluid flow in porous sandstones: *Petrophysical properties*: American Association of Petroleum Geologists Bulletin, v. 78, p. 355–377.  
Bruhn, R. L., 1993, Crack 2D: An unpublished MatLab computer program for deriving permeability tensors in two dimensions using the methods of Oda, 1986 and Oda et al., 1987: University of Utah, Department of Geology and Geophysics, Structural Geology Lab.  
Bruhn, R. L., Yonke, W. E., and Parry, W. T., 1990, Structural and fluid-chemical properties of seismogenic normal faults: *Tectonophysics*, v. 175, p. 139–157.  
Bruhn, R. L., Parry, W. T., Yonke, W. A., and Thompson, T., 1994, Fracturing and hydrothermal alteration in normal fault zones: *PAGEOPH*, v. 142, p. 609–644.  
Byerlee, J., 1993, Model for episodic flow of high-pressure water in fault zones before earthquakes: *Geology*, v. 21, p. 303–306.  
Caine, J. S., Coates, D. R., Timofeev, N. P., and Davis, W. D., 1991, Hydrogeology of the Northern Shawangunk Mountains: New York State Geological Survey Open-File Report Ig806, 72 p. and maps.  
Caine, J. S., Forster, C. B., and Evans, J. P., 1993, A classification scheme for permeability structures in fault zones: *Eos (Transactions, American Geophysical Union)*, v. 74, p. 677.  
Chester, F. M., and Logan, J. M., 1986, Composite planar fabric of gouge from the Punchbowl fault, California: *Journal of Structural Geology*, v. 9, p. 621–634.  
Chester, F. M., Evans, J. P., and Biegel, R. L., 1993, Internal structure and weakening mechanisms of the San Andreas fault: *Journal of Geophysical Research*, v. 98, p. 771–786.  
Davison, C. C., and Wang, C. Y., 1988, Hydrogeologic characteristics of major fracture zones in a large granite batholith of the Canadian shield: Proceedings, 4th Canadian-American Conference on Hydrogeology, Banff, Canada, June 1988, n.p.  
Evans, J. P., 1990, Textures and deformation mechanisms and the role of fluids in cataclastically deformed granitic rocks, in Knipe, R. J., and Rutter, E. eds., *Deformation mechanisms, rheology, and tectonics*: Geological Society of London Special Publication 54, p. 29–39.  
Forster, C. B., and Evans, J. P., 1991, Hydrogeology of thrust faults and crystalline thrust sheets: Results of combined field and modeling studies: *Geophysical Research Letters*, v. 18, p. 979–982.  
Forster, C. B., Goddard, J. V., and Evans, J. P., 1994, Permeability structure of a thrust fault, in *The mechanical involvement of fluids in faulting*: U.S. Geological Survey Open-File Report 94-228, p. 216–223.  
Goddard, J. V., and Evans, J. P., 1995, Chemical changes and fluid-rock interaction in faults of crystalline thrust sheets, northwestern Wyoming, U.S.A.: *Journal of Structural Geology*, v. 17, p. 533–547.  
Moore, J. C., and Vrolijk, P., 1992, Fluids in accretionary prisms: *Reviews of Geophysics*, v. 30, p. 113–135.  
Newman, J., and Mitra, G., 1994, Fluid-influenced deformation and recrystallization of dolomite at depth on low temperatures along a natural fault zone, Mountain City window, Tennessee: *Geological Society of America Bulletin*, v. 106, p. 1267–1280.  
Oda, M., Hatsuyma, Y., and Ohnishi, Y., 1987, Numerical experiments on permeability tensor and its application to jointed granite at Stripa mine, Sweden: *Journal of Geophysical Research*, v. 92, p. 8037–8048.  
Oliver, J., 1986, Fluids expelled tectonically from orogenic belts: Their role in hydrocarbon migration and other geologic phenomena: *Geology*, v. 14, p. 99–102.  
Parry, W. T., and Bruhn, R. L., 1986, Pore fluid and seismogenic characteristics of fault rock at depth on the Wasatch fault, Utah: *Journal of Geophysical Research*, v. 91, p. 730–744.  
Parry, W. T., Wilson, P. N., and Bruhn, R. L., 1988, Pore-fluid chemistry and chemical reactions on the Wasatch normal fault, Utah: *Geochimica et Cosmochimica Acta*, v. 52, p. 2053–2063.  
Randolph, L., and Johnson, B., 1989, Influence of faults of moderate displacement on groundwater flow in the Hickory sandstone aquifer in central Texas: *Geological Society of America Abstracts with Programs*, v. 21, p. 242.  
Scholz, C. H., 1987, Wear and gouge formation in brittle faulting: *Geology*, v. 15, p. 493–495.  
Scholz, C. H., 1990, *The mechanics of earthquakes and faulting*: Cambridge, Cambridge University Press, 439 p.  
Scholz, C. H., and Anders, M. H., 1994, The permeability of faults, in *The mechanical involvement of fluids in faulting*: U.S. Geological Survey Open-File Report 94-228, p. 247–253.  
Sibson, R. H., 1977, Fault rocks and fault mechanisms: *Geological Society of London Journal*, v. 133, p. 191–231.  
Sibson, R. H., 1981, Fluid flow accompanying faulting: Field evidence and models, in Simpson, D. W., and Richards, P. G., eds., *Earthquake prediction—An international review*: American Geophysical Union Monograph, Maurice Ewing Series, v. 4, p. 593–603.  
Smith, L., Forster, C. B., and Evans, J. P., 1990, Interaction of fault zones, fluid flow, and heat transfer at the basin scale, in *Hydrogeology of permeability environments*: International Association of Hydrogeologists, v. 2, p. 41–67.

Manuscript received March 8, 1996

Revised manuscript received July 10, 1996

Manuscript accepted July 29, 1996